Optical properties of a three-dimensional chiral metamaterial*

Juan-Juan Guo(郭娟娟), Mao-Sheng Wang(汪茂胜)†, and Wan-Xia Huang(黄万霞)

College of Physics and Electronic Information, Anhui Normal University, Wuhu 241000, *China*

(Received 4 June 2017; revised manuscript received 6 September 2017; published online 20 November 2017)

A three-dimensional chiral metamaterial with four-fold rotational symmetry is designed, and its optical properties are investigated by numerical simulations. The results show that this chiral metamaterial has the following features: high polarization conversion, perfect circular dichroism, and asymmetric transmission of circularly polarized light. A comparison of the results of chiral metamaterials without and with weak coupling between the constituent nanostructures enables us to confirm that the optical properties of our proposed nanostructure are closely related to the coupling between the single nanoparticles. This means that the coupling between nanoparticles can enhance the polarization conversion, circular dichroism, and asymmetric transmission. Due to the excellent optical properties, our metamaterial might have potential applications in the development of future multi-functional optical devices.

Keywords: chiral metamaterial, polarization conversion, circular dichroism, asymmetric transmission

PACS: 42.70.–a, 81.05.Xj **DOI:** 10.1088/1674-1056/26/12/124211

1. Introduction

The term chiral describes an object, especially a molecule, which lacks any plane of mirror symmetry. That is to say, a chiral material will never coincide exactly with the mirror image of itself in any orientation. Optical activities occur only in chiral materials, but they are not significant in natural chiral materials. Metamaterials are artificially designed and can exhibit electromagnetic responses that are not observed in naturally occurring materials. In recent years, a new class of metamaterial, known as chiral metamaterial (CM), has attracted much attention due to its optical properties. For example, polarization conversion (PC),[1–6] circular dichroism (CD),[7–9] and asymmetric transmission (AT)[10–14] in CM have been studied intensively. Because of their these fascinating properties, CMs are widely used in many areas such as in circular polarizers,[15] ultrasensitive detection, characterization of biomolecules,[16,17] nanomotors,[18,19] and optofluidic sorters.[20] Negative refraction of chiral metamaterials, which was first identified by Pendry, has also been extensively investigated.[21–23] Moreover, the polarization properties of light propagated through metamaterial slabs were systematically analyzed by the method of advanced Jones calculus by Menzelet in 2010.[24] The PC and CD have also been investigated in the metamaterials with the chiral symmetry breaking.[25,26] A complementary helical metamaterial with strong circular conversion dichroism was reported in Ref. [27], and it will be a good candidate for controlling wavefront with high efficiency. Although many studies have focused on chiral metamaterials, the chiral metamaterials with multiple functions have been rarely investigated.

In this study, a three-dimensional (3D) chiral metamaterial composed of four identical z-like-shaped nanoparticles (ZLSNs) is designed. The unit cell of this chiral metamaterial has a four-fold rotation symmetry. We demonstrate numerically the optical properties of this 3D chiral metamaterial. The simulated results show that the PC, circular-difference response (CDR) for linear polarized light, and AT for circularly polarized light are generated at 1515.8 nm. Due to the twists between the ZLSNs, the couplings between ZLSNs are relatively strong. To reveal the effects of coupling on the chiral metamaterial's optical properties, we study the optical properties of two types of chiral metamaterials, i.e., those without or with weak coupling between the nanostructures. A comparison of their properties indicates that the PC, CDR, and AT of the proposed chiral metamaterial originate mainly from the coupling of nanoparticles in the unit cell. The proposed chiral metamaterial has a simple geometry and it can be potentially employed to fabricate devices such as a polarization controller, optical diode, and multifunction devices.

2. Structures and method

Figures 1(a) and 1(b) schematically show the unit cell and its array for a chiral material, respectively. Four identical ZLSNs are arranged on the substrate and act as the building blocks of the array. Here, the unit cell possesses the fourfold rotational symmetry. Each ZLSN in the unit cell is composed of two Ag arms and one Ag base that are orthogonal to each other. The long side's length a (b or c) of the bottom (middle or top) bar is set to be 200 nm. The short side lengths w and t of the bars are both fixed at 60 nm. The spacing S between

*Project supported by the National Natural Science Foundation of China (Grant No. 11304002), the Natural Science Foundation of Education Bureau of Anhui Province, China (Grant No. KJ2013A136), and the Natural Science Foundation of Anhui Province, China (Grant No. 1208085MA07).

†Corresponding author. E-mail: wangms@mail.ahnu.edu.cn

© 2017 Chinese Physical Society and IOP Publishing Ltd

nearest-neighbor Ag bases is 300 nm. The periods are the same in both x and y directions: both are P, and P is 600 nm, unless otherwise specified. The linearly polarized plane wave normally illuminates the structure from the positive or negative direction on the z-axis side. In order to obtain a comprehensive understanding of the electromagnetic (EM) response of the ZLSN array, numerical simulation is performed by the finite difference time domain (FDTD) method. In the numerical modeling, the permittivity of silver is described by the Drude model with the plasma frequency $\omega_p = 1.374 \times 10^{16}$ rad/s and the collision frequency $\gamma = 1.224 \times 10^{14}$ rad/s, and the dielectric constant of the glass substrate (SiO_2) is set to be 2.25.

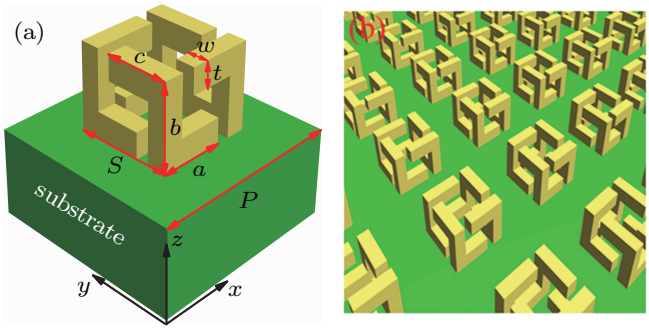


Fig. 1. (color online) Schematic diagrams for (a) unit cell and (b) its array of the 3D chiral metamaterial.

3. Results and discussion

To quantitatively analyze the transmission and reflection of an EM wave normally incident on the C_4-CM along both the positive and negative z directions, firstly, we briefly introduce some fundamentals. It is assumed that the polarized incident wave propagates along the z direction. In the matrix form, the transmission coefficient can be presented as follows:

$$\begin{pmatrix} E_t^x \\ E_t^y \end{pmatrix} = \begin{pmatrix} t_{xx\pm} & t_{xy\pm} \\ t_{yx\pm} & t_{yy\pm} \end{pmatrix} \begin{pmatrix} E_i^x \\ E_i^y \end{pmatrix} = T_{\text{lin}\pm} \begin{pmatrix} E_i^x \\ E_i^y \end{pmatrix}, \tag{1}$$

where $T_{\text{lin}\pm}$ is the Jones matrix.[24] The subscript '+' or '–' indicates the propagation EM wave along the positive or negative direction of the z axis, respectively. The element t_{xy+} indicates the ability of a structure to transform a y-polarized incident wave, which is along the positive direction of the z axis, into an x-polarized transmitted wave. Other elements in the Jones matrix are similar to t_{xy+}. Then, the circularly polarized transmitted waves for linear polarized incident wave can be presented as follows:

$$\begin{aligned} \begin{pmatrix} E_t^{\text{RCP}} \\ E_t^{\text{LCP}} \end{pmatrix} &= \begin{pmatrix} E_t^x + \text{j}E_t^y \\ E_t^x - \text{j}E_t^y \end{pmatrix} = \begin{pmatrix} t_{\text{RCP}x\pm} & t_{\text{RCP}y\pm} \\ t_{\text{LCP}x\pm} & t_{\text{LCP}y\pm} \end{pmatrix} \begin{pmatrix} E_i^x \\ E_i^y \end{pmatrix} \\ &= T_{\text{CL}\pm} \begin{pmatrix} E_i^x \\ E_i^y \end{pmatrix}, \end{aligned} \tag{2}$$

$$\begin{aligned} T_{\text{CL}\pm} &= \begin{pmatrix} t_{\text{RCP}x\pm} & t_{\text{RCP}y\pm} \\ t_{\text{LCP}x\pm} & t_{\text{LCP}y\pm} \end{pmatrix} \\ &= \frac{1}{\sqrt{2}} \begin{pmatrix} t_{xx\pm} + \text{j}t_{yx\pm} & t_{xy\pm} + \text{j}t_{yy\pm} \\ t_{xx\pm} - \text{j}t_{yx\pm} & t_{xy\pm} - \text{j}t_{yy\pm} \end{pmatrix}, \end{aligned} \tag{3}$$

where RCP and LCP represent right circularly polarized and left circularly polarized waves, respectively. The $T_{\text{CL}\pm}$ is the linear polarized wave–circularly polarized wave transmission matrix. The constant $1/\sqrt{2}$ is the normalization coefficient, and the element $t_{\text{RCP}x+}$ indicates the ability of a structure to transform an x-polarized incident wave, which is along the positive direction of the z axis, into an RCP transmitted wave. Other elements in matrix $T_{\text{CL}\pm}$ are similar to $t_{\text{RCP}x+}$. Furthermore, the transmission matrix for circularly polarized wave to circularly polarized wave is given by

$$T_{\text{Circ}\pm} = \begin{pmatrix} t_{\text{RR}\pm} & t_{\text{RL}\pm} \\ t_{\text{LR}\pm} & t_{\text{LL}\pm} \end{pmatrix} = \frac{1}{2} \begin{pmatrix} [t_{xx\pm} + t_{yy\pm}] + \text{j}\,[t_{xy\pm} - t_{yx\pm}] & [t_{xx\pm} - t_{yy\pm}] - \text{j}\,[t_{xy\pm} + t_{yx\pm}] \\ [t_{xx\pm} - t_{yy\pm}] + \text{j}\,[t_{xy\pm} + t_{yx\pm}] & [t_{xx\pm} + t_{yy\pm}] - \text{j}\,[t_{xy\pm} - t_{yx\pm}] \end{pmatrix}, \tag{4}$$

where t_{RR}, t_{RL}, t_{LR}, and t_{LL} are the transmission coefficients, and R and L denote RCP wave and LCP waves, respectively.

For the proposed chiral structure with a fourfold rotational symmetry, the amplitude and phase of zero-order transmission spectrum, i.e., the matrix elements of $T_{\text{lin}\pm}$ versus frequency, are simulated and depicted in Fig. 2. As illustrated in Fig. 2, the co-polarized transmission coefficients are equal for the incident wave that is x (or y)-polarized along the positive (or negative) z axis. The amplitudes of cross-polarized transmission coefficients are equal, but their phases meet the conditions: $\varphi_{yx\pm} = \pm\pi + \varphi_{xy\pm}$ and $\varphi_{yx\mp} = \pm\pi + \varphi_{yx\pm}$. These results show that

$$t_{xx-} = t_{yy-} = t_{xx+} = t_{yy+}, \quad t_{yx-} = -t_{xy-} = -t_{yx+} = t_{xy+}. \tag{5}$$

The transmission amplitude $|t_{xx\pm}|$ (or $|t_{yy\pm}|$) dip appears at 1515.8 nm and its value is about 0.37. The polarization conversion spectra $|t_{yx\pm}|$ (or $|t_{xy\pm}|$) shows a peak at the same wavelength and the value is about 0.58. In fact, the transmission characteristics are related to the current oscillation configurations excited in the metamaterial structure. For example, the current vector distribution at 1515.8 nm for the y-polarized incident wave along the negative z axis is depicted in Fig. 3. Due to the coupling between the top (i.e., positive z direction) and bottom (i.e., negative z direction) bars which are parallel to the y axis, their currents are anti-parallel, the total transmission fields with the y polarization show destructive interference, and a dip in the transmission amplitude $|t_{yy-}|$ appears. Under the excitation due to the current of the bars parallel to

the y axis, the electrons move along the ZLSNs to the bars parallel to the x axis and result in currents parallel with the x axis. Finally, the total transmission fields with the x polarization show constructive interference, and then, the peak in the transmission amplitude $|t_{xy-}|$ appears.

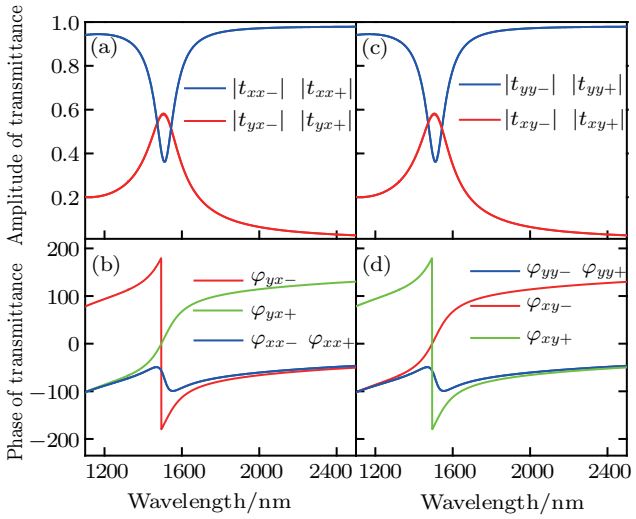


Fig. 2. (color online) Simulated zero-order transmission amplitude spectra for ((a) and (b)) x-polarization and ((c) and (d)) y-polarization incident waves along different propagation directions.

Combining Eqs. (3) and (5), we can obtain

$$t_{\mathrm{RCP}y-} = \mathrm{j}t_{\mathrm{RCP}x-} = \mathrm{j}t_{\mathrm{LCP}y+} = t_{\mathrm{LCP}x+},$$

$$t_{\mathrm{LCP}y-} = -\mathrm{j}t_{\mathrm{LCP}x-} = -\mathrm{j}t_{\mathrm{RCP}x+} = t_{\mathrm{RCP}y+}. \quad (6)$$

According to Eq. (3), the elements of linear/circularly polarized conversion matrix can be calculated. Here, the simulated $t_{\mathrm{RCP}x-}$, $t_{\mathrm{RCP}y-}$, $t_{\mathrm{LCP}x-}$, and $t_{\mathrm{LCP}y-}$ are depicted in Fig. 4. One can observe that the amplitudes of the transmission coefficients have the following relationships:

$$\begin{aligned} |t_{\mathrm{RCP}x-}| &= |t_{\mathrm{RCP}y-}|, \quad \varphi_{\mathrm{RCP}y-} - \varphi_{\mathrm{RCP}x-} = 90^{\mathrm{o}}, \\ |t_{\mathrm{LCP}x-}| &= |t_{\mathrm{LCP}y-}|, \quad \varphi_{\mathrm{LCP}x-} - \varphi_{\mathrm{LCP}y-} = 90^{\mathrm{o}}. \end{aligned} \quad (7)$$

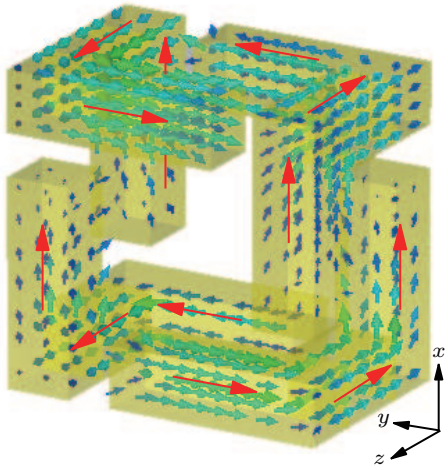


Fig. 3. (color online) Current distribution for y-polarized incident wave at 1515.8 nm.

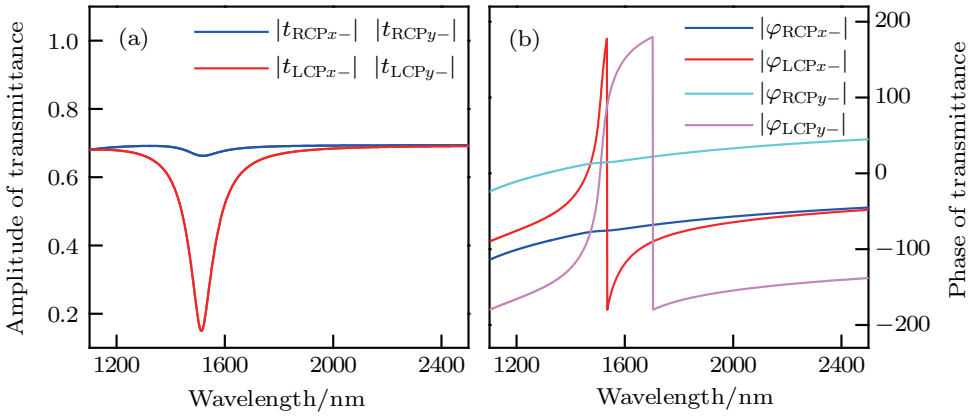


Fig. 4. (color online) Plots of (a) amplitude of transmittance and (b) phase of transmittance versus wavelength for linear-polarization/circular-polarization transmission coefficients $t_{\mathrm{RCP}x-}$, $t_{\mathrm{RCP}y-}$, $t_{\mathrm{LCP}x-}$, and $t_{\mathrm{LCP}y-}$.

Equations (7) and (6) are in agreement with each other. At 1515.8 nm, $|t_{\mathrm{RCP}x-}|$ (or $|t_{\mathrm{RCP}y-}|$) has a resonance dip of about 0.663, and $|t_{\mathrm{LCP}x-}|$ (or $|t_{\mathrm{LCP}y-}|$) has a resonance dip of about 0.149. This means that the RCP/LCP responses of the chiral metamaterial from the x-polarized wave propagating along the z axis are different. To investigate the influences of the nanostructure on RCP and LCP, CDR, which is an important index to measure the chirality of material, is introduced [28]

$$\mathrm{CDR} = \frac{I_{\mathrm{LCP}} - I_{\mathrm{RCP}}}{(I_{\mathrm{LCP}} + I_{\mathrm{RCP}})/2}, \quad (8)$$

where I_{LCP} and I_{RCP} are the transmission intensities associated with LCP and RCP excitation, respectively. The CDR can take values between -2 ($I_{\mathrm{LCP}} = 0$) and 2 ($I_{\mathrm{RCP}} = 0$). The CDR is associated with CD, which is the difference in absorbance between the LCP and RCP light. In the case of x (or y)-polarized incident wave, CDRs for the negative z axis (red curve) and positive z axis (blue curve) are displayed in Fig. 5. The CDR+ (or CDR-) has a maximum 1.81 (or minimum -1.81) value at a resonant wavelength of 1515.8 nm. The results show that when the x (or y)-polarized incident wave propagates through the chiral metamaterial, RCP and LCP are both induced. At the resonant wavelength, the RCP light is dominant for the

positive z axis incident x (or y)-polarized wave, and *vice versa*.

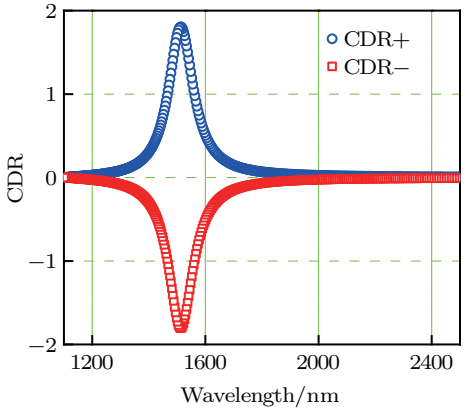


Fig. 5. (color online) CDRs for negative z axis (red curve) and positive z axis (blue curve) to x (or y)-polarized incident wave.

When our proposed chiral metamaterial is normally illuminated by an RCP or LCP wave, the matrix connecting the incident and transmitted circularly polarized components can be derived by combining Eqs. (4) and (5). Further, this matrix can be described as follows:[7,18,29]

$$T_{\mathrm{Circ}\pm} = \begin{pmatrix} t_{\mathrm{RR}\pm} & t_{\mathrm{RL}\pm} \\ t_{\mathrm{LR}\pm} & t_{\mathrm{LL}\pm} \end{pmatrix} = \begin{pmatrix} t_{xx\pm} - \mathrm{j}t_{yx\pm} & 0 \\ 0 & t_{xx\pm} + \mathrm{j}t_{yx\pm} \end{pmatrix}. \quad (9)$$

The squares of these elements correspond to transmission and circularly polarized conversion in terms of power. Thus, the circularly polarized conversion of our proposed chiral metamaterial is $|t_{\mathrm{RL}\pm}|^2 = |t_{\mathrm{LR}\pm}|^2 = 0$. For normally incident RCP (or LCP) wave, there will be no LCP (or RCP) light in the transmission wave. Furthermore, the numerical results of $I_{\mathrm{RR}-} = |t_{\mathrm{RR}-}|^2$ and $I_{\mathrm{RR}+} = |t_{\mathrm{RR}+}|^2$ are shown in Fig. 6. It is obvious that $I_{\mathrm{RR}+} \neq I_{\mathrm{RR}-}$, which indicates the AT effect of circular polarization of our proposed chiral metamaterial. Here, the AT effect, similar to the nature of the diode, for circularly polarized wave is characterized by Δ, which could be defined as the difference between the transmittances in the two opposite propagation directions (positive/negative z axis). Thus, the degree of AT can be expressed as follows:

$$\Delta = I_{\mathrm{RR}+} - I_{\mathrm{RR}-}. \quad (10)$$

Figure 6 shows that for the normal incident RCP wave, the transmittance indicates a resonant wavelength of 1515.8 nm; $I_{\mathrm{RR}+}$ has a very small dip, while $I_{\mathrm{RR}-}$ has a substantial dip. The difference between $I_{\mathrm{RR}+}$ and $I_{\mathrm{RR}-}$ reaches 0.832 at the resonant wavelength, which indicates a big AT effect for RCP. It is evident that the corresponding results of LCP are very similar to those of RCP, and will not be described here.

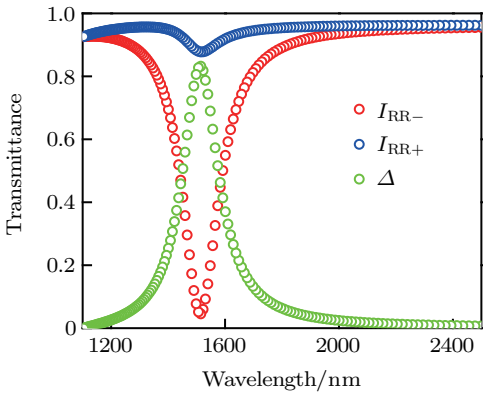


Fig. 6. (color online) Variations of transmittances with wavelength for $I_{\mathrm{RR}-}$ (blue curve) and $I_{\mathrm{RR}+}$ (red curve) of circularly/circularly polarized light in two opposite propagation directions (positive/negative z axis) and for the degree of AT Δ (green curve) for circularly/circularly polarized light.

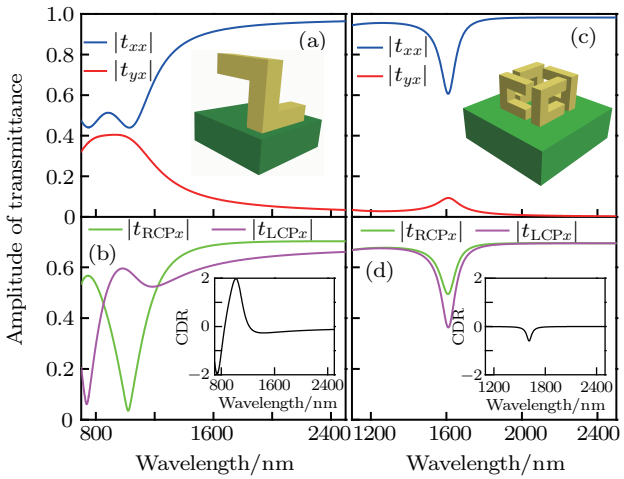


Fig. 7. (color online) ((a) and (c))Simulated zero-order transmission amplitudes $|t_{xx}|$ and $|t_{yx}|$ for two kinds of chiral metamaterials. The insets in panels (a) and (c) show the sketch maps of the corresponding unit cell. The corresponding linear/circularly polarized conversions $|t_{\mathrm{RCP}x}|$ and $|t_{\mathrm{LCP}x}|$ are displayed in panels (b) and (d), respectively. The insets in panels (b) and (d) show the corresponding CDR.

In order to reveal the influence of the coupling between the ZLSNs on the PC, we simulate the optical properties of two other kinds of chiral metamaterials, whose unit cells are shown in the insets in Figs. 7(a) and 7(c). Without loss of generality, the incident light propagates along the positive z axis and the subscript "+" is omitted. Figure 7(a) presents the simulated zero-order transmission amplitudes $|t_{xx}|$ and $|t_{yx}|$ for the chiral metamaterial whose unit cell contains a single ZLSN. In addition, the corresponding simulated results $t_{\mathrm{RCP}x}$ and $t_{\mathrm{LCP}x}$ are depicted in Fig. 7(b). Here, the period P is 300 nm and the other parameters are the same as those mentioned above. Compared with the PC and CDR of the coupled ZLSNs, those (i.e., $|t_{yx}|$ in Fig. 7(a) and CDR in the inset of Fig. 7(b)) of a single ZLSN are evidently weak for incident light at the corresponding wavelength (around 1515.8 nm). Figure 7(c) presents the simulated zero-order transmission amplitudes $|t_{xx}|$ and $|t_{yx}|$ for the chiral metamaterial whose unit cell contains

four U-like-shaped nanoparticles with four-fold rotation symmetry. The parameters are the same as those mentioned above with $P = 600$ nm. Moreover, the corresponding simulated results $t_{\mathrm{RCP}x}$ and $t_{\mathrm{LCP}x}$ are depicted in Fig. 7(d). One can see that its PC and CDR (inset in Fig. 7(d)) are also significantly smaller than those of the coupled ZLSNs. Therefore, the coupling between ZLSNs can enhance the PC and CDR.

4. Conclusions

In this work, we study the optical properties of four-fold rotation symmetry metamaterials, whose unit cell consists of four ZLSNs. A substantial PC, near-perfect CDR, and AT of linear/circularly polarized incident light are observed. In order to study the coupling effect, we study the optical properties of two kinds of chiral metamaterials, i.e., those without and with weak coupling between the nanostructures. The results show that the coupling between nanostructures can enhance the values of PC, CDR, and AT of chiral metamaterials. The results of our study will open the way for novel plasmonic material design for a wide range of applications, e.g., in life science microscopy and in polarization controllers and optical diodes. Moreover, our metamaterials can be employed to fabricate multifunctional optical devices and can reduce the space and cost of optical devices.

References

[1] Ren M, Plum E, Xu J and zheludev N I 2012 *Nat. Commun.* **3** 833
[2] Plum E, Liu X X, Fedotov V A, Chen Y, Tsai D P and Zheludev N I 2009 *Phys. Rev. Lett.* **102** 113902
[3] Rogacheva A V, Fedotov V A, Schwanecke A S and Zheludev N I 2006 *Phys. Rev. Lett.* **97** 177401
[4] Yang Z J, Hu D J, Gao F H and Hou Y D 2016 *Chin. Phys. B* **25** 084201
[5] Wu S, Zhang Z, Zhang Y, Zhang K, Zhou L, Zhang X and Zhu Y 2013 *Phys. Rev. Lett.* **110** 207401
[6] Shao J, Li J, Wang Y H, Li J Q, Dong Z G and Zhou L 2016 *Chin. Phys. B* **25** 058103
[7] Li W, Coppens Z J, Besteiro L V, Wang W Y, Govorov A O and Valentine J 2015 *Nat. Commun.* **6** 8379
[8] Decker M, Klein M W, Wegener M and Linden S 2007 *Opt. Lett.* **32** 856
[9] Abdulrahman N A, Fan Z, Tonooka T, Kelly S M, Gadegaard N, Hendry E, Govorov A O and Kadodwala M 2012 *Nano Lett.* **12** 977
[10] Pfeiffer C, Zhang C, Ray V, Guo L J and Grbic A 2014 *Phys. Rev. Lett.* **113** 023902
[11] Menzel C, Helgert C, Rockstuhl C, Kley E B, Tünnermann A, Pertsch and Lederer F 2010 *Phys. Rev. Lett.* **104** 253902
[12] Plum E, Fedotov V A and Zheludev N I 2009 *Appl. Phys. Lett.* **94** 131901
[13] Fedotov V A, Mladyonov P L, Prosvirnin S L, Rogacheva A V, Chen Y and Zheludev N I 2006 *Phys. Rev. Lett.* **97** 167401
[14] Huang L, Fan Y H, Wu S and Yu L Z 2015 *Chin. Phys. Lett.* **32** 094101
[15] Gansel J K, Thiel M, Rill M S, Decker M, Bade K, Saile V, von Freymann G, Linden S and Wegener M 2009 *Science* **325** 1513
[16] Hendry E, Carpy T, Johnston J, Popland M, Mikhaylovskiy R V, Lapthorn A J, Kelly S M, Barron L D, Gadegaard N and Kadodwala M 2010 *Nat. Nanotechnol.* **5** 783
[17] Hentschel M, Schäferling M, Weiss T, Kuball H G, Liu N and Giessen H W 2012 *Nano Lett.* **12** 2542
[18] Liu M, Zentgraf T, Liu Y, Bartal G and Zhang X 2010 *Nat. Nanotechnol.* **5** 570
[19] Kim K, Xu X, Guo J and Fan D L 2014 *Nat. Commun.* **5** 3632
[20] Tkachenko G and Brasselet E 2014 *Nat. Commun.* **5** 3577
[21] Zhang S, Park Y, Li J, Lu X, Zhang W and Zhang X 2009 *Phys. Rev. Lett.* **102** 023901
[22] Plum E, Zhou J, Dong J, Fedotov V A, Koschny T, Soukoulis C M and Zheludev N I 2009 *Phys. Rev. B* **79** 035407
[23] Pendry J B 2004 *Science* **306** 1353
[24] Menzel C, Rockstuhl C and Lederer F 2010 *Phys. Rev. A* **82** 053811
[25] Husu H, Canfield B K, Laukkanen J, Bai B, Kuittinen M, Turunen J and Kauranen M 2008 *Appl. Phys. Lett.* **93** 183115
[26] Huang W X, Zhang Y, Tang X M, Cai L S, Zhao J W, Zhou L, Wang Q J, Huang C P and Zhu Y Y 2011 *Opt. Lett.* **36** 3359
[27] Wang Z K, Yang Z Y, Tao H and Zhao M 2016 *Acta Phys. Sin.* **65** 217802 (in Chinese)
[28] Hassey R, Swain E J, Hammer N I, Venkataraman D and Barnes M D 2006 *Science* **314** 1437
[29] Ye Y and He S 2010 *Appl. Phys. Lett.* **96** 203501